Organically Modified Transition−Metal Oxide Mesoporous Thin Films and Xerogels

ARTICLE *in* CHEMISTRY OF MATERIALS · DECEMBER 2004

Impact Factor: 8.35 · DOI: 10.1021/cm048559b

2 AUTHORS:

Paula C. Angelomé
Comisión Nacional de Energía Atómica
24 PUBLICATIONS **685** CITATIONS
SEE PROFILE

Galo J A A Soler-Illia
National University of General San Martín
144 PUBLICATIONS **8,180** CITATIONS
SEE PROFILE

Organically Modified Transition-Metal Oxide Mesoporous Thin Films and Xerogels

Paula C. Angelomé and Galo J. de A. A. Soler-Illia*

Unidad de Actividad Química, Centro Atómico Constituyentes, CNEA, Av. Gral Paz 1499 (B1650KNA) San Martín, Pcia de Buenos Aires, Argentina

Received August 27, 2004. Revised Manuscript Received October 27, 2004

Organic molecules have been incorporated into the pore system of mesoporous TiO_2 and ZrO_2 xerogels and thin films. Surface-modifying functions include alkyl, aryl, amino, sulfonate, thiol, and polyol. Phosphate, phosphonate, carboxylate, and polyphenol were used as grafting groups. The incorporation of these functions into the mesoporous network (typically 2−8 μmol/m^2) was monitored by crossing FTIR and EDS. In particular, the cases of dihexadecyl phosphate, monododecyl phosphate, 3-nitrophthalic acid, TIRON (disodium 1,2-dihydroxybenzene, 3,5-disulfonate), and thiol-bearing carboxylates are discussed. Uptake experiments suggest that the pore structure plays a key role in the accessibility of the pore system. Leaching experiments in different solvents and conditions were performed to assess the anchoring of the grafted functions. This permits tailoring of the molecule grafting, from firmly anchored functions to groups with controlled lability.

Introduction

A decade after the seminal works of the Mobil group in the synthesis of mesoporous (MP) silica,[1] there is nowadays a sound library of synthesis protocols for mesoporous oxides and non-oxides.[2,3] A step beyond is the incorporation of organic groups within mesoporous phases, leading to precisely located chemical functions in controlled size accessible cavities. This subject is being increasingly studied, to be able to design multifunctional materials. A great deal of work has been performed in silica mesoporous matrixes[4−8] with organic functions either attached to the pore surface[9] or embedded in the pore walls.[10] These studies were mostly conducted on mesoporous powders. On the other hand, less work has been performed in thin mesoporous functionalized films, which present great interest, due to their high potential as advanced coatings (sensors, adsorbents, smart glasses, ...).[11−17] Organically modified mesoporous transition-metal oxides (MTMOs) have been less studied.[18,19] These are particularly interesting because of the electronic properties of the inorganic skeleton, which could be modified by their interaction with included or grafted organic molecules, leading to a great variety of potential applications (magnetic,

* To whom correspondence should be addressed. E-mail: gsoler@cnea.gov.ar.

(1) Kresge, C. T.; Leonowicz, M. E.; Roth, W. J.; Vartuli, J. C.; Beck, J. S. *Nature* **1992**, *359*, 710.
(2) Soler-Illia, G. J. d. A. A.; Sanchez, C.; Lebeau, B.; Patarin, J. *Chem. Rev.* **2002**, *102*, 4093.
(3) Soler-Illia, G. J. d. A. A.; Crepaldi, E. L.; Grosso, D.; Sanchez, C. *Curr. Opin. Colloid Surf. Sci.* **2003**, *8*, 109.
(4) Stein, A.; Melde, B.; Schroden, R. C. *Adv. Mater.* **2000**, *12*, 1403.
(5) Moller, K.; Bein, T. *Chem. Mater.* **1998**, *10*, 2950.
(6) Sayari, A.; Hamoudi, S. *Chem. Mater.* **2001**, *13*, 3151.
(7) Shi, J.; Hua., Z.; Zhang, L. *J. Mater. Chem*, **2004**, *14*, 795.
(8) Lim, M. H.; Stein, A. *Chem. Mater.* **1999**, *11*, 3285.
(9) (a) Macquarrie, D. J.; Jackson, D. B.; Tailland, S.; Utting, K. A. *J. Mater. Chem.* **2001**, *11*, 1843. (b) Maschmeyer, T.; Rey, F.; Sankar, G.; Thomas, J. M. *Nature* **1995**, *378*, 159. (c) Brunel, D.; Cauvel, A.; Fajula, F.; Di Renzo, F. *Stud. Surf. Sci. Catal.* **1995**, *97*, 173. (d) Brunel, D. *Microporous Mesoporous Mater.* **1999**, *27*, 239. (e) Anwander, R. *Chem. Mater.* **2001**, *13*, 4419. (f) Burkett, S.; Sims, S. D.; Mann, S. *Chem. Commun.* **1996**, 1367. (g) MacQuarrie, D. J. *Chem. Commun.* **1996**, 1961. (h) Shepard, D. S.; Zhou, W.; Maschmeyer, T.; Matters, J. M.; Roper, C. L.; Parsons, S.; Johnson, B. F. G.; Duer, M. J. *Angew. Chem., Int. Ed.* **1998**, *37*, 2719. (i) Richer, R.; Mercier, L. *Chem. Mater.* **2001**, *13*, 2999.
(10) (a) Inagaki, S.; Guan, S.; Fukushima, Y.; Ohsuna, T.; Terasaki, O. *J. Am. Chem. Soc.* **1999**, *121*, 9611. (b) Melde, B. J.; Holland, B. T.; Blanford, C. F.; Stein, A. *Chem. Mater.* **1999**, *11*, 3302. (c) Asefa, T.; MacLachlan, M. J.; Coombs, N.; Ozin, G. A. *Nature* **1999**, *402*, 867. (d) Yoshina-Ishii, C.; Asefa, T.; Coombs, N.; MacLachlan, M. J.; Ozin, G. A. *Chem. Commun.* **1999**, 2539. (e) Asefa, T.; MacLachlan, M. J.; Grondley, H.; Coombs, N.; Ozin, G. A. *Angew. Chem., Int. Ed.* **2000**, *39*, 1808. (f) Asefa, T.; Yoshina-Ishii, C.; MacLachlan, M. J.; Ozin, G. A. *J. Mater. Chem.* **2000**, *10*, 1751. (g) Lu, Y.; Fan, H.; Doke, N.; Loy, D. A.; Assink, R. A.; La Van D. A.; Brinker, C. J. *J. Am. Chem. Soc.* **2000**, *122*, 5258. (h) Inagaki, S.; Guan, S.; Ohsuna, T; Terasaki, O. *Nature* **2002**, *416*, 304.
(11) Sanchez, C.; Soler-Illia, G. J. d. A. A.; Ribot, F.; Grosso, D. *C. R. Chim.* **2003**, *6*, 1131.
(12) Grosso, D.; Cagnol, F.; Soler-Illia, G. J. d. A. A.; Crepaldi, E. L.; Amenitsch, H.; Brunet-Bruneau, A.; Bourgeois, A.; Sanchez, C. *Adv. Funct. Mater.* **2004**, *14*, 309.
(13) (a) Alonso, B.; Balkenende, A. R.; Albouy, P.-A.; Durand, D.; Babonneau, F. *New J. Chem.* **2002**, *26*, 1270. (b) Alonso, B.; Balkenende, A. R.; Albouy, P.-A.; Amenitsch, H.; Rager, M.-N., Babonneau, F. *J. Sol-Gel Sci. Technol.* **2003**, *26*, 587. (c) Balkenende, A. R., De Theije, F. K.; Kriege, J. C. K. *Adv. Mater.* **2003**, *15*, 139.
(14) Wong, E. M.; Markowitz, M. A.; Qadri, S. B., Golledge, S.; Castner, D. G.; Gaber, B. P. *J. Phys. Chem B* **2002**, *106*, 6652.
(15) Liu, N.; Assink, R. A.; Smarsly, B.; Brinker, C. J. *Chem. Commun.* **2003**, 1146; Liu, N.; Dunphy, D. R.; Atanassov, P.; Bunge, S. D.; Chen, Z.; López, G. P.; Boyle, T. J.; Brinker, C. J. *Nano Lett.* **2004**, *4*, 551.
(16) Subbiah, S.; Mokaya, R. *Chem. Commun.* **2003**, 860.
(17) Petkov, N.; Mintova, S.; Jean, B.; Metzger, T.; Bein, T. *Mater. Sci. Eng., C* **2003**, *23*, 827.
(18) (a) Crepaldi, E. L.; Soler-Illia, G. J. d. A. A.; Grosso, D.; Albouy, P.-A.; Sanchez, C. *Chem. Commun.* **2001**, 1582. (b) Angelomé, P. C.; Aldabe-Bilmes, C.; Calvo, M. E.; Crepaldi, E. L.; Grosso, D.; Sanchez, C.; Soler-Illia, G. J. de A. A. *New. J. Chem.* **2005**, *29*, in press.
(19) Coakley, K. M.; Liu, Y.; McGehee, M. D.; Frindell, K.; Stucky, G. D. *Adv. Funct. Mater.* **2003**, *13*, 301.

10.1021/cm048559b CCC: $30.25
Published on Web 12/16/2004

optoelectronic, and photovoltaic materials). Another potentially interesting application of organically modified MTMOs is in controlled release devices (particularly for nontoxic TiO_2). Mesoporous silica is mostly modified by organosilane molecules, and incorporation of other molecules into the mesopore system has been achieved mostly by physisorption. On the contrary, a great variety of anchoring groups with different complexing abilities can be used to graft organic functions to MTMO surfaces, therefore providing a wide range of possibilities.

MTMO can be efficiently produced by evaporation-induced self-assembly (EISA) methods as xerogels, powders, films, or fibers with high surface areas (100−500 m^2/g), a variety of mesostructures (2D or 3D hexagonal, cubic, local, ...), and amorphous or nanocrystalline walls.[20−28] A subsequent modification of the MTMO pore surface creates spatially separated well-defined functionalities, important for advanced applications (sensors, actuators, optoelectronic materials, controlled delivery devices, ...). The simplest approach is to postfunctionalize an MTMO by grafting organic or organometallic groups. However, the routes to multifunctional MTMOs are not straightforward, and particular attention has to be paid to aspects such as surface chemistry, diffusion within pores, dissolution, etc. Another important issue is the integrity of modified MTMOs under solvent flux (i.e, function leaching), due to the fact that functions are grafted via coordination and noncovalent bonds to the pore wall.

In this work, titania and zirconia mesoporous films or xerogels with a 2D hexagonal (*p*6*mm*) or *Im*3*m* cubic mesostructure were prepared by EISA, using a triblock copolymer template (Pluronics F127). Control dense films were produced in the absence of templates. Mesoporous nanocrystalline coatings obtained upon heating ($T > 350$ °C) present high organization, excellent optical quality, and thermal stability (Figure 1a). Organic molecules presenting complexing grafting groups (carboxylate, dicarboxylate, polyphenol, phosphate, ...) and diverse functions (hydrophobic (alkyl or aryl chains), hydrophilic (amine, sulfonic acids), metallophilic (thiol)) were explored as surface modifiers. The incorporation of these functions into the mesoporous network was monitored by crossing FTIR, EDS, and chemical analysis. Leaching experiments in different solvents and conditions were performed to assess the anchoring of the grafted groups. Experiments performed in films presenting different mesostructures (i.e., cubic versus 2D hexagonal) show different trends regarding pore accessibility and the possibility of functionalization.

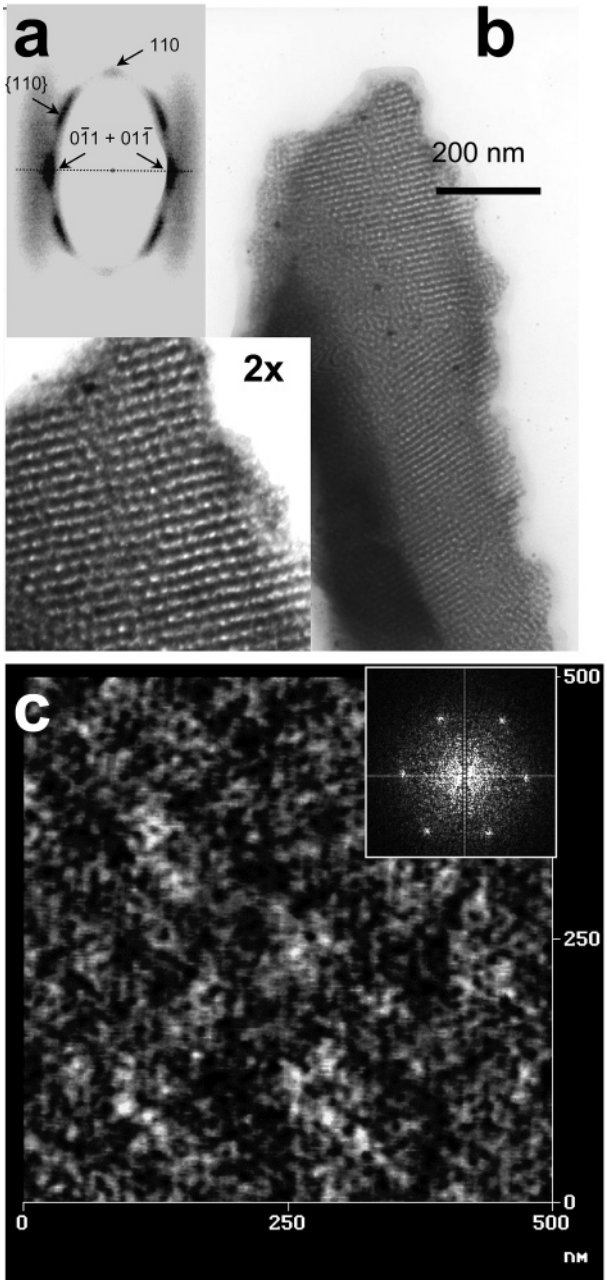

Figure 1. (a) 2D SAXS pattern of a ZrO_2 thin mesoporous film treated at 130 °C. The indexed spot pattern corresponds to a distorted *Im*3*m* cubic mesostructure; the dotted line represents the film orientation. (b) TEM image (projection along the [110] axis) of a TiO_2 *Im*3*m* cubic film used in this work. (c) AFM image of a calcined titania mesoporous film. Inset: FFT of the AFM image, showing the 4 + 2 periodicity corresponding to the [110] face of a cubic arrangement.

Experimental Section

Mesostructured Materials Preparation. Mesoporous xerogels or thin films were prepared by EISA, under controlled deposition conditions (*T*, RH), as previously reported.[21−24] Initial solutions were prepared by mixing $TiCl_4$ or $ZrCl_4$ in ethanol. Nonionic triblock copolymer Pluronic F127 ($(EO)_{106}(PO)_{70}(EO)_{106}$) was used as a structure-directing agent. Chlorides were slowly added under stirring to alcoholic solutions containing templates. Water ($h = [H_2O]/[M] = 10$ for titania based solids, $h = 20$ for zirconia based

(20) Crepaldi, E. L.; Soler-Illia, G. J. d. A. A.; Grosso, D.; Cagnol, F.; Ribot, F.; Sanchez, C. *J. Am. Chem. Soc.*, **2003**, *125*, 9770 and references therein.
(21) Grosso, D.; Soler-Illia, G. J. d. A. A.; Babonneau, F.; Sanchez, C.; Albouy, P.-A.; Brunet-Bruneau, A.; Balkenende, A. R. *Adv. Mater.* **2001**, *13*, 1085.
(22) (a) Yang, P.; Zhao, D.; Margolese, D. I.; Chmelka, B. F.; Stucky, G. D. *Nature* **1998**, *395*, 583. (b) Yang, P.; Zhao, D.; Margolese, D. I.; Chmelka, B. F.; Stucky, G. D. *Chem. Mater.* **1999**, *11*, 2813.
(23) Soler-Illia, G. J. d. A. A.; Sanchez, C. *New J. Chem.* **2000**, 493.
(24) Crepaldi, E. L.; Soler-Illia, G. J. d. A. A.; Grosso, D.; Sanchez, C. *New J. Chem.* **2003**, *27*, 9.
(25) Soler-Illia, G. J. d. A. A.; Scolan, E.; Louis, A.; Albouy, P. A.; Sanchez, C. *New J. Chem.* **2001**, *25*, 156.
(26) Frindell, K. L.; Bartl, M. H.; Popitsch, A.; Stucky, G. D. *Angew. Chem., Int. Ed.* **2002**, *41*, 959.
(27) Alberius, P. C. A.; Frindell, K. L.; Hayward, R. C.; Kramer, E. J.; Stucky, G. D.; Chmelka, B. F. *Chem. Mater.* **2002**, *14*, 3284.
(28) Choi, S. Y.; Mamak, M.; Coombs, N.; Chopra, N.; Ozin, G. A. *Adv. Funct. Mater.* **2004**, *14*, 335.

Scheme 1

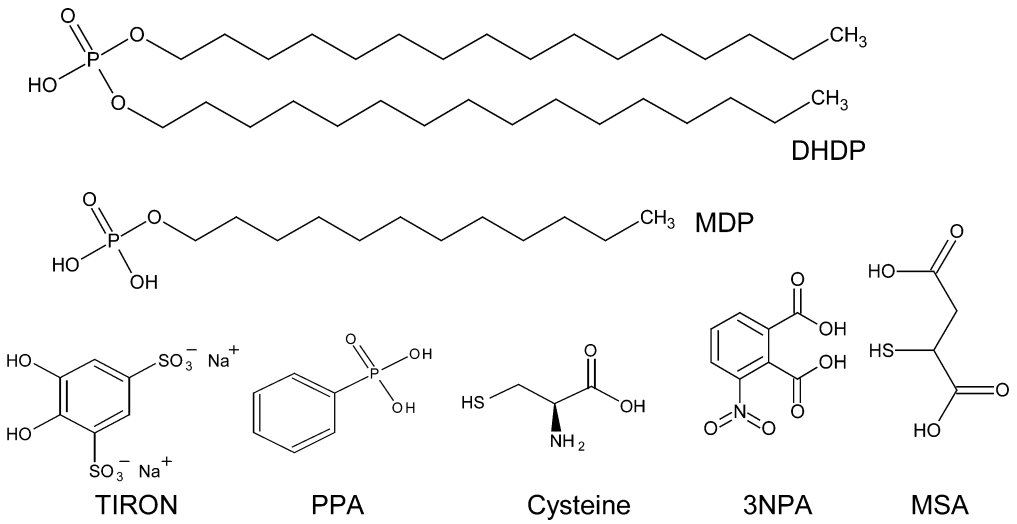

solids) was subsequently added under stirring. The final molar ratio in solution was M/template/H_2O/EtOH = 1/0.005/*h*/40. Clean glass, silicon wafers, polymer sheets (cellulose acetate), or KBr pressed pellets were used as substrates.

Titania films and xerogels are produced by evaporation under controlled humidity conditions (RH > 40%).[20,21] Zirconia films were prepared by a two-step method, similar to the one previously described for zirconia-based mesoporous films:[18] dip-coating performed under a dry atmosphere (RH < 10%) followed by a short exposure (10−20 s) to water vapor. Nonmesoporous (i.e., dense) films and xerogels were produced using the same precursor mixtures in the absence of templates, for control experiments. As-prepared films were submitted to subsequent 48 h treatments at 10% or 50% RH and 60 and 135−200 °C to improve cross-linking of the inorganic network, and favor microphase separation. Thermal treatment of these stabilized coatings (up to 350 °C, 3 h dwell time) was performed in tubular ovens, under still air, using 1 °C min^{-1} temperature ramps. Alternatively, templates can be removed from mesostructured films stabilized at 200 °C by treatment in slightly acidic ethanol solutions (0.01 mol dm^{-3} HCl).

Molecules used for grafting (Scheme 1) were chosen to show the inclusion of varied organic functions (alkyl, aryl, thiol, sulfonate, amino), with different anchoring groups (phosphate, phosphonate, polyhydroxyaromatic, carboxylate, dicarboxylate). Molecules forming intensely colored complexes with Ti centers (TIRON (disodium 1,2-dihydroxybenzene, 3,5-disulfonate)) or long aliphatic chain molecules (dihexadecyl phosphate (DHDP), monododecyl phosphate (MDP)) were selected for the kinetics experiments to optimize the UV/vis or FTIR signals. A typical functionalization experiment was performed by dipping a calcined mesoporous film previously rinsed with ethanol in a continuously stirred 0.01 mol/dm^3 solution of the chosen molecule in THF, acetone, or water (the solvent depends on the functionalizer's solubility). The immersion time (t_{uptake}) was varied from 5 min to several days. After immersion, the film was rinsed several times with the appropriate solvent and dried in air. Care has to be taken in adequately rinsing and eventually carefully rubbing the film surface, as SEM/EDS analysis of substituted films shows that, in some cases, small quantities of the organic compound remain in the film surface after washing, leading to detection of organic matter which is not included within the pore system.

Leaching experiments were performed by introducing a functionalized film with a given t_{uptake} in an appropriate solvent with stirring. Leaching was evaluated from 5 min to several days by analyzing the UV or FTIR spectra of the films.

Characterization. To completely characterize the mesostructures, 2D SAXS experiments were performed at the SAXS line in the Laboratório Nacional de Luz Síncrotron (LNLS), Campinas, SP, Brazil, using $\lambda = 1.608$ Å and a sample−detector distance of 650 mm; image plates were used as detectors. Obtained peak positions were in excellent agreement with those obtained for cubic *Im*3*m* or *p*6*mm* mesostructures in former work.[20,21,24,29] XRD patterns corresponding to the out-of-plane planes (i.e., pore planes parallel to the substrate) were collected in $\theta-2\theta$ mode using a conventional goniometer, Siemens D5000 (Cu $K\alpha_1$ radiation). TEM images were collected using a Philips EM 301 transmission microscope (CMA, Universidad de Buenos Aires (UBA), Argentina) operated at 65 kV. Samples were obtained by scratching the films from the substrate and deposited on Formvar-coated copper or gold grids.

FTIR spectra were recorded by transmission using a Nicolet Magna 560 instrument, equipped with a liquid nitrogen cooled MCT-A detector. Samples were mostly ground and embedded in KBr pellets. An alternative method consisted in depositing a mesoporous film on a KBr pellet, and performing all consolidation, thermal treatment, and functionalization steps on this pellet-supported thin film. This procedure results in a significant FTIR signal enhancement. UV/vis measurements were carried out in a Hewlett-Packard 8453 UV/vis spectrophotometer. Films were placed directly in the sample holder (identical films were used as blanks, to avoid interference effects due to film thickness), and quartz cells were used for solution analysis.

EDS was performed in a Philips SEM microscope equipped with EDAX. AFM measurements were conducted in tapping mode under an air atmosphere, in a Nanoscope III apparatus, at CMA-UBA.

Ellipsometry measurements were carried out with a variable-angle spectroscopic ellipsometer using porous or dense (control) MO_2 films deposited onto silicon substrates. Optical parameters (thickness, *e*, and refractive index, *n*) were estimated by fitting the obtained ellipsometric ψ and Δ quantities. The refractive index was modeled according to a Maxwell−Garnett effective medium approximation, to take into account pores (inclusions) within a matrix.[30] MP cubic TiO_2 films present a refraction index of $n = 1.660$, and for ZrO_2 films, $n = 1.71-1.72$, irrespectively of their mesostructure (*p*6*mm* or *Im*3*m*). The refraction index of the walls, $n_{TiO_2} = 2.18$, and $n_{ZrO_2} = 1.993$, was assumed equal to that obtained

(29) Soler-Illia, G. J. d. A. A.; Crepaldi, E. L.; Grosso, D.; Durand, D.; Sanchez, C. *Chem. Commun.* **2002**, 2298.
(30) Maxwell−Garnett, J. C. *Philos. Trans. R. Soc.* **1906**, *203*, 385.

for nonporous films subjected to the same treatment. Thus, the porosity of the ZrO_2 and TiO_2 samples is estimated to be 25−33% and 42%, respectively.

Results and Discussion

Mesostructure Characterization. Under the synthesis conditions used, titania films or xerogels presenting cubic *Im*3*m* mesostructure ($a = 190$ Å for fresh films) are obtained, in good agreement with previous work.[20] Upon thermal treatment, XRD patterns of films show peaks at $2\theta = 1.4-1.9°$ (corresponding to the d_{110} distance of the *Im*3*m* cubic phase, now distorted by a uniaxial shrinkage in the *z* direction), depending on the sample pretreatment and calcination temperature, as has been observed before;[24,31] xerogels show less marked peak shifts ($2\theta = 0.9-1.0°$ for calcined samples) due to a more uniform shrinkage.[32] Figure 1 shows typical TEM and AFM images of a TiO_2 film. AFM measurements show a typical pattern, consisting in six pores surrounding a central pore, four of them at shorter distances (∼170 Å) and two of them farther away (ca. 190 Å ≈ *a*); the ratio between both distances is 0.89.[33] This "4 + 2" arrangement has been often confused with a hexagonal pattern,[19] but actual values are close to those corresponding to the [110] face of the *Im*3*m* mesophase, which is parallel to the substrate (ratio of 0.86). Xerogel and film surface areas present typical values of 150 m^2/g upon thermal treatment to 350 °C, as assessed by nitrogen adsorption.[20] Zirconia films can be obtained as 2D hexagonal (*p6mm*)[18] or cubic (*Im*3*m*) mesostructures (Figure 1a) by aging freshly synthesized films under different RH conditions (i.e., 10% or 50%, respectively) for several days.[34,35] Both mesoporous zirconia films present high uniaxial contraction ($2\theta = 2-2.5°$ for those calcined to 350 °C). The film thickness and porosity were obtained from ellipsometry measurements. Typical thickness values are in the 100−300 nm (for films deposited at room temperature and a withdrawal speed of 1 cm s^{-1}, and calcined up to 350 °C, which are the usual conditions, otherwise stated); the thickness increases slightly with increasing withdrawal speed, and decreases with increasing sol temperature. The porosity of these films is estimated to be 42−46% of the total volume from ellipsometry.[36]

Uptake Experiments. Calcined mesoporous films were used as substrates for molecule incorporation. EDS, FTIR, and UV/vis spectroscopy have been used to assess the incorporation of organic functions into mesopores qualitatively and semiquantitatively. Figure 2 presents UV/vis spectra of TiO_2 cubic films, which were treated with a 10^{-2} mol dm^{-3} aqueous TIRON solution for 3 h. An intense absorption band at 450 nm is observed in a TiO^{2+}−TIRON solution (Figure 2, curve a), due to the LMCT transition of a Ti−TIRON complex. In the case of films exposed to TIRON, an intense absorption is observed at close wavelengths in MP titania (Figure 2, curve b), but no significant absorption is observed for nontemplated films (Figure 2, curve c). This leads to the conclusion that a significantly larger number of Ti−O surface sites are available and accessible in cubic mesoporous titania films than in dense ones. Coincidently, EDS analysis of TIRON-substituted mesoporous TiO_2 films yields 5.2 ± 0.4% S/Ti (Table 1). This value corresponds to ca. 4 μmol of S/m^2 (i.e., 2 μmol of TIRON/m^2), in good agreement with grafting values found in mesoporous powders.[6] No significant S signal is observed in the EDS spectra of the dense film.

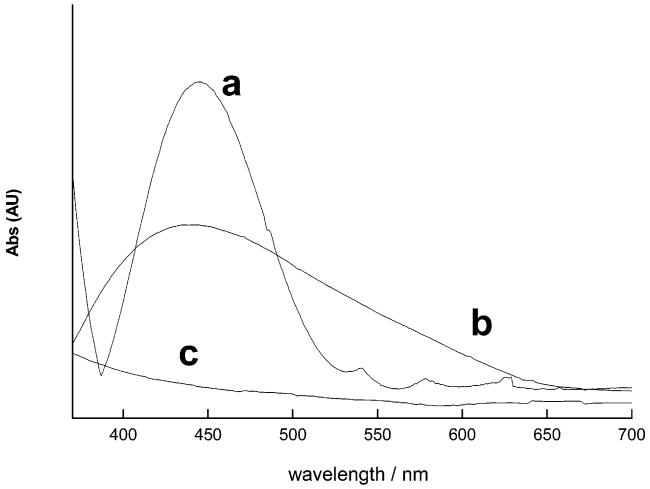

Figure 2. UV/vis spectra of the TIRON−Ti complex (a) and TIRON-substituted cubic MP (b) and non-MP (c) titania films.

Table 1. Percentage of Heteroatom Content Obtained in Functional Mesoporous TiO_2 Films by EDS, for $t_{uptake} = 1$ h in 0.01 mol dm^{-3} Solutions of Different Functionalizers

functionalizer	% heteroatom
Cys	3.0
DHDP	5.5
MDP	16.6
MSA	7.6
PPA	9.0
TA	6.3
TIRON	5.8

The same differences in the organic uptake between mesoporous and dense films are observed for DHDP (Figure 3a); FTIR spectra of films exposed to DHDP solutions in THF show intense bands (ν_{C-H} in the 2900−3000 cm^{-1} region, $\nu_{P=O}$ between 1100 and 1300 cm^{-1}, ν_{P-O-C} in the 1000−1100 cm^{-1} region, band assignment in Table 2); this constitutes evidence of an important incorporation of DHDP molecules into the mesoporous films. Bands corresponding to water (ν_{O-H} large band at 3500 cm^{-1}, δ_{O-H} band at 1600 cm^{-1}, partially overlapping the δ_{P-OH} band centered at 1650 cm^{-1} in the reference DHDP spectrum) and to the inorganic framework ($\nu_{Ti-O-Ti} < 700$ cm^{-1}) are also observed.[37] The phosphate bands ($\nu_{P=O}$, ν_{P-O-R}, ν_{P-O-C}) are overlapped in

(31) Grosso, D.; Soler-Illia, G. J. d. A. A.; Crepaldi, E.; Cagnol, F.; Sinturel, C.; Bourgeois, A.; Brunet-Bruneau, A.; Amenitsch, H.; Albouy, P.-A.; Sanchez, C. *Chem. Mater.* **2003**, *15*, 4562.
(32) Soler-Illia, G. J. d. A. A.; Scolan, E.; Louis., A.; Albouy, P.-A.; Sanchez, C. *New J. Chem.* **2001**, *25*, 156.
(33) Angelomé, P. C.; Ludueña, S.; Pietrasanta, L.; Soler-Illia, G. J. d. A. A. Work in progress.
(34) Crepaldi, E. L.; Soler-Illia, G. J. d. A. A.; Bouchara, A.; Grosso, D.; Durand, D.; Sanchez, C. *Angew. Chem., Int. Ed.* **2003**, *42*, 347.
(35) Soler-Illia, G. J. d. A. A.; Crepaldi, E. L.; Grosso, D.; Sanchez, C. *J. Mater. Chem.* **2004**, *14*, 1879.
(36) The studied MP TiO_2 films present a refraction index $n = 1.66$. Assuming amorphous titania walls, with refraction index estimated as $n_{TiO_2} = 2.18$, porosity can thus be estimated as 42−46% of the total volume, assuming the Bruggeman or the Maxwell−Garnet approximation.
(37) Socrates, G. *Infrared and Raman Characteristic Group Frequencies*, 3rd ed.; John Wiley and Sons: Chichester, U.K., 2001.

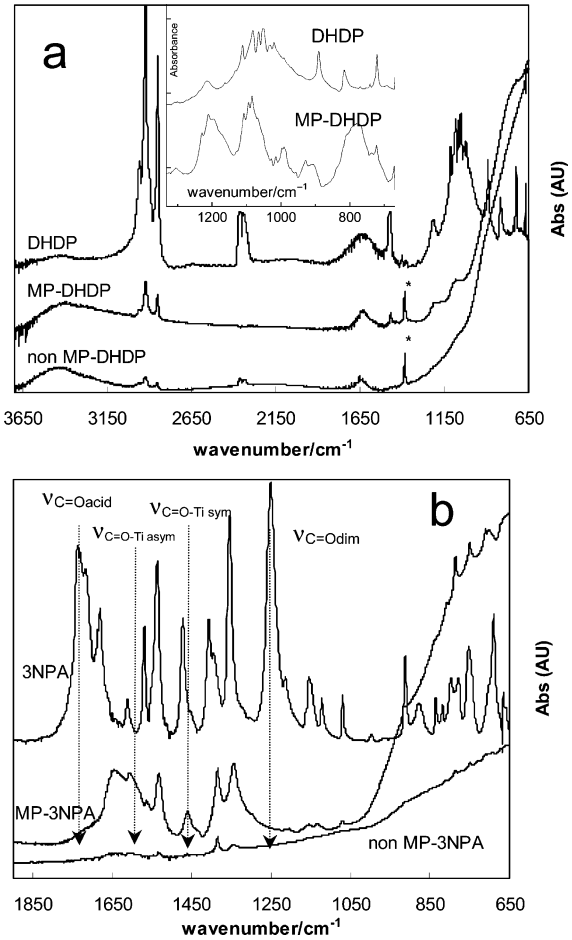

Figure 3. FTIR spectra of pure molecules and substituted titania MP and non-MP films: (a) DHDP and DHDP-substituted TiO_2 films (the inset shows details of the 800−1200 cm^{-1} region that contains phosphate bands); (b) 3NPA and 3NPA-substituted titania films in the 650−1800 cm^{-1} range (the loss of the acid peak and the rise of carboxylate−Ti coordination bands can be observed upon fnctionalization).

the 900−1200 cm^{-1} range, and the complete assignment of the phosphate−titania interactions requires a careful analysis. However, it can be observed that a peak pattern arises in the 900−1000 cm^{-1} range for substituted films (zone of P−O−C and P−OH bands), which is different from the bands observed in pure DHDP (Figure 3a, inset). Previous work in related systems suggests that these bands could be due to P−OH−Ti interaction.[38] Moreover, the water deformation band at 1600 cm^{-1} is symmetrical, and no P−OH contribution is observed. This suggests that the phosphate groups are attached to the TiO_2 surface by complexation. In comparison, nonmesoporous samples display significantly lower or insignificant FTIR signals. These data are confirmed by EDS (Table 1).[39] Signals found in 2D hexagonal MP ZrO_2 films (low intensity for FTIR bands of DHDP−ZrO_2 and MDP−ZrO_2) are much weaker than the ones obtained in TiO_2 MP films for an equivalent t_{uptake} (see below).[40]

(38) (a) Guerrero, G.; Mutin, P. H.; Vioux, A. *Chem. Mater.* **2001**, *11*, 4367. (b) Tejedor-Tejedor, M. I.; Anderson, M. A. *Langmuir* **1990**, *6*, 602.

(39) As stated in the Experimental Section, a thorough SEM/EDS analysis shows that no DHDP crystals are present on the mesoporous film surface.

(40) This led us to choose titania cubic films to study in depth the uptake and leaching processes. Zirconia behavior will be compared when necessary.

Table 2. Band Assignment of the FTIR Spectra Presented in Figure 3

functionalization with DHDP	band position (cm^{-1}) DHDP	MP DHDP	non-MP DHDP
C−H sym str vib	2850	2850	2850
C−H asym str vib	2920	2920	2920
P−OH def vib	1750		
$(CH_2)_n$ def vib	1470	1470	
P═O str	850−1200	850−1200	
P−O−R asym str	850−1200	850−1200	
P−O−C asym str vib	850−1200	850−1200	
Ti−O str vib		650−1000	650−1000
functionalization with 3NPA	**3NPA**	**MP 3NPA**	**non-MP 3NPA**
OH str	3150		
C═O str vib	1735		
CO asym str bident/ bridging complexes		1605	∼1600
NO_2 asym str	1536	1532	1534
CO sym str bident/ bridging complexes		1459	
C−O str + OH def vib	1407		
NO_2 sym str	1354	1343	1343
C−O str (dimer)	1250		
aromatic ring with three substituents	<750	<750	<750
Ti−O str vib		650−1000	650−1000

Carboxylate anchoring groups are indeed bound to the titania surface. FTIR spectra of 3-nitrophthalic acid (3NPA) incorporated into mesoporous films (Figure 3b) show that the C═O bands corresponding to the acid functions of the free molecule ($\nu_{C=O}$ = 1735 cm^{-1}, $\nu_{C=O\ dimer}$ = 1250 cm^{-1}) are replaced by two bands (1459 and 1605 cm^{-1}, corresponding to the symmetric and asymmetric $\nu_{C=O}$ modes, respectively) characteristic of bidentate or bridging carboxylate−Ti bonding ($\Delta\nu$ = 146 cm^{-1}).[41] These experiments demonstrate that the existence of a pore system with high surface area is determinant in the incorporation of the organic molecules, and that the cubic pore system is accessible to organic molecules. This is reinforced by the EDS data obtained in mesoporous titania films substituted with several P-containing or S-containing functional molecules, which are in the range of 3−9% atom/Ti (see Table I); in all cases, the heteroatom content is negligible (i.e., less than the noise threshold) in nonmesoporous films. Therefore, it can be concluded that different grafting groups such as phosphate, phosphonate, polyhydroxyaromatic, or carboxylate are useful to link different organic functions (alkyl, aryl, thiol, ...).

Uptake Kinetics. Figure 4a shows the uptake of DHDP with time (followed by FTIR) in titania (300 nm thick, 42% porosity assessed by ellipsometry) and zirconia (450−470 nm thick, 25−33% porosity for both mesostructures, assessed by ellipsometry) MP thin films calcined to 350 °C. In the case of cubic TiO_2 or ZrO_2, molecule uptake occurs in two steps; 80% of the organic molecules are incorporated within the first 5 min. The remaining 20% are gradually incorporated, and saturation is reached in about 80 min. Incorporation curves present the same shape irrespectively of the film thickness, and data can be superimposed on a master curve

(41) Soler-Illia, G. J. d. A. A.; Boggiano, M. K.; Rozes, L.; Turrin, C.-O.; Caminade, A.-M.; Majoral, J.-P.; Sanchez, C. *Angew. Chem., Int. Ed.* **2000**, *39*, 4249 and references therein.

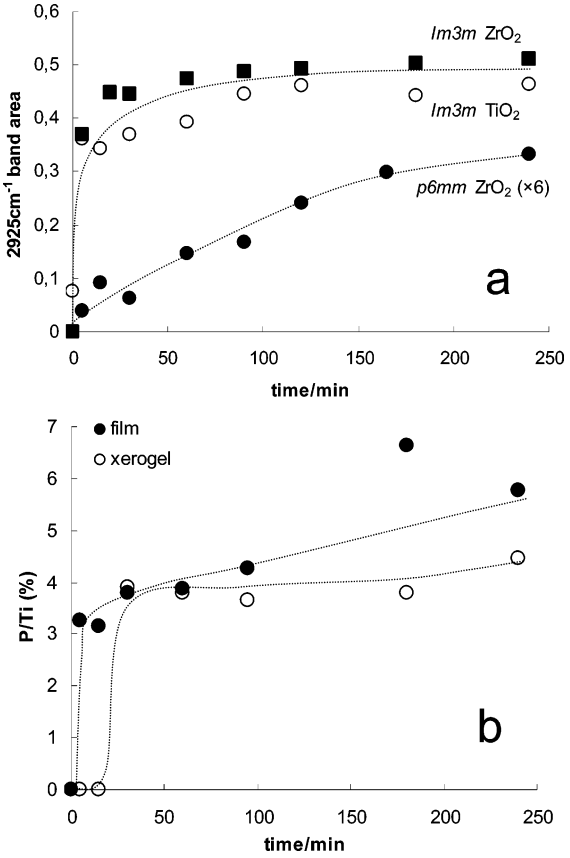

Figure 4. (a) Time dependence of DHDP incorporation (0.01 mol dm^{-3} solution in THF) into MP cubic titania (○) and zirconia (■) films and MP 2D hexagonal zirconia films (●) as assessed by FTIR. (b) Time dependence of DHDP incorporation (0.01 mol dm^{-3} solution in THF) into MP titania films (●) and 2 μm xerogel particles (○), as assessed by EDS. Dotted lines are a guide to the eye.

when normalized to the maximum uptake (Supporting Information). This demonstrates that adsorption kinetics does not seem to play a fundamental limitation role in molecule incorporation into *thin mesoporous cubic films*. DHDP uptake depends almost linearly on film thickness (see the Supporting Information); this suggests that DHDP diffusion is fast along the cubic film, and that DHDP molecules can sample the whole film thickness within short times. In the case of MP 2D hexagonal ZrO_2 films, two features are observed: (a) incorporation is lower at equivalent times, for films with equivalent thicknesses and porosities; (b) a slow but continuous increase in DHDP incorporation is observed (reaching ca. 20% of the maximum uptake for a cubic film in 24 h). This result can be attributed to either a lower quantity of sites or a more difficult accessibility of DHDP molecules into the bidimensional pore system. Previous work has demonstrated that copolymer-templated cubic or 2D hexagonal mesoporous powders present similar surface areas irrespectively of the mesostructure,[20,22,27,31] ruling out the first hypothesis. Thus, the open 3D frameworks derived from the *Im*3*m* mesostructures should be more accessible to entering molecules than the 2D hexagonal channels parallel to the substrate, as has been previously suggested in the literature. Apart from a 3D structure, pore interconnection in the cubic framework seems to be the key to an efficient molecule transport for film functionalization. Indeed, previously synthesized 3D copolymer-templated silica presents closed porosity structures.[42] Thus, to achieve accessibility, initially unconnected pores have to merge, leading to an open pore structure. Such interconnections are possible thanks to (a) residual wall microporosity, which is favored in polymer-templated mesostructures,[3] and (b) the formation of necks between pores, related to the mesostructure shrinkage produced at high temperatures. The latter factor is critically dependent on the mesostructure symmetry. While uniaxial contraction may lead to interconnection in *Im*3*m* mesostructures,[31] it only leads to deformation in the parallel channels which constitute the *p*6*mm* pore arrays. Thus, thermal treatment may play a major role in accessibility when the mesostructure symmetry permits pore fusion. Related results in silica and titania films suggest that the postsynthesis and thermal treatment steps during template elimination are critical to attain pore accessibility.[43]

In the case of titania xerogels, diffusion effects influence the inclusion of the functional molecules, as has been found in silica MP powders.[44] Figure 4b shows the time dependence of DHDP incorporation into titania MP films and xerogels, assessed by SEM/EDS. Incorporation into small particles derived from xerogels (ca. 2 μm) is significantly slower than incorporation into thin films ($\tau_{1/2} = 5$ and 60 min, respectively), and presents a sigmoidal shape, instead of the decelerative curves observed for thin films. Indeed, for 10 μm particles, DHDP incorporation is even slower, as $\tau_{1/2} >$ 240 min. The longer times required to homogeneously incorporate organic functions in xerogels suggest that on a larger length scale of the solids ($\sim$1$-$10 μm), pore filling depends on molecule transport inside the pore system, apart from diffusion from solution. Similar features are observed in the case of other phosphate-grafted molecules, such as MDP. Another important aspect is the response of a mesoporous gel to thermal treatment. In the absence of a substrate, pore shrinkage is averaged. As a consequence, the strong pore merging (consequence of a uniaxial contraction of about 50$-$70% in the *z* axis) that occurs in thin films is absent. As a consequence, pore interconnection might be lower in xerogels than in films, particularly at lower thermal treatment temperatures. Pore interconnection should also depend critically on the nature of the inorganic wall, and its behavior under thermal evolution. Systematic experiments comparing titania and zirconia films and gels are under way to clarify these issues.

From these results, it can be advanced that two main limitations to DHDP incorporation arise: (i) pore accessibility (related to the symmetry and connectivity of the pore array) and (ii) transport within the pore system. The latter factor can be explained in terms of molecule diffusion (with the limitations imposed by the diffusion of a molecule commensurate with the pore size)[45] but also molecule/wall interactions. This latter factor seems important, and interactions have been recently identified as a key factor in the modification of small-molecule diffusion coefficients within

(42) Yu, K.; Smarsly, B.; Brinker, C. J. *Adv. Funct. Mater.* **2003**, *13*, 47.
(43) Grosso, D.; Sanchez, C. Work in progress, private communication.
(44) Díaz, J. F.; Balkus, K. J., Jr.; Bedioui, F.; Kurshev, V.; Kevan, L. *Chem. Mater.* **1997**, *9*, 61.
(45) Maldonado, A.; Nicot, C.; Waks, M.; Ober, R.; Urbach, W.; Langevin, D. *J. Phys. Chem. B* **2004**, *108*, 2893.

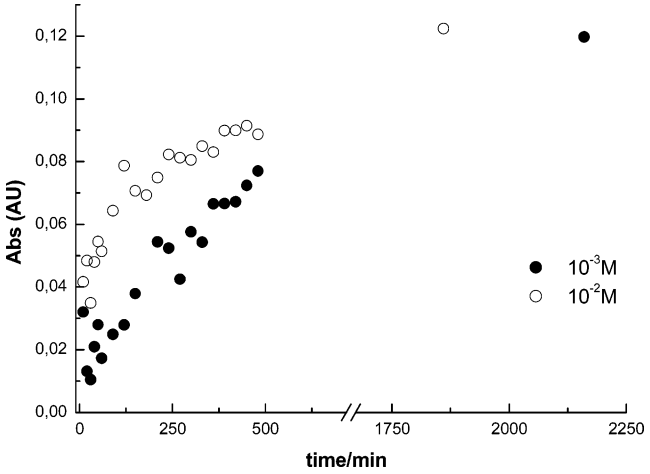

Figure 5. Time dependence of TIRON incorporation (open circles, 10^{-3} mol dm^{-3} solution in water; full circles, 10^{-2} mol dm^{-3} solution in water) into MP titania films, as assessed by UV.

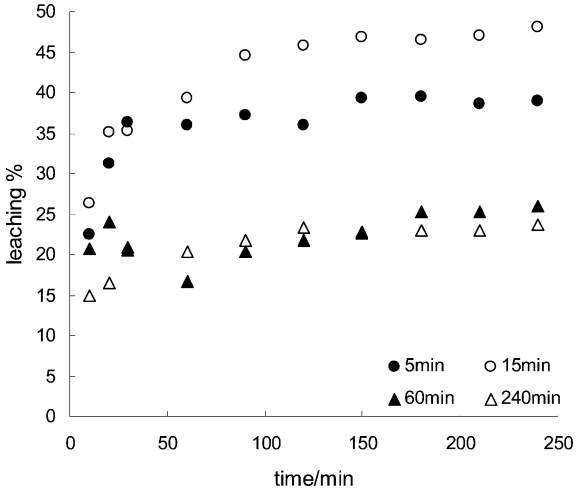

Figure 6. Time dependence of function leaching (in THF) of DHDP from titania cubic films submitted to functionalization for different periods, t_{uptake} = 5 min (full circles), 15 min (open circles), 60 min (full triangles), and 240 min (open triangles).

Table 3. Leaching Percentage of Different Functionalizers from TiO_2 Mesoporous Films

functionalizer	solvent	% leaching (4 h)	followed by
MDP	THF	10	FTIR
DHDP	H_2O	0	FTIR
DHDP	$CHCl_3$	15	FTIR
DHDP	THF	23	FTIR
TIRON	H_2O, pH 5.5	30	UV/vis
TIRON	H_2O, pH 3	65	UV/vis
3NPA	H_2O, pH 5.5	45	UV/vis

the pore system of functionalized mesoporous silica.[46,47] Earlier work in postfunctionalized 2D hexagonal silica powders demonstrated that silane functional groups were concentrated in the outer surface and near the pore openings; this is possible when the grafting reaction is fast (relative to transport to the pore interior) and almost irreversible, which should be the case for silanes postgrafted onto silica pore surfaces.[8] In the case of TiO_2 mesoporous materials, the stability of the DHDP−Ti complex should be responsible for the slow incorporation into xerogels, and similar results are expected, albeit the phosphate−Ti complexation interaction is more reversible than the formation of a Si−O−Si bond. We propose that transport of the grafting molecule to the inner pores follows a sequence of adsorption−desorption−diffusion. Hence, a higher complexation ability of the grafting group should result in slower incorporation of the organic function. The solvent also plays an important role, particularly favoring the desorption step. Experiments are being performed at present to separate the intrinsic effects of the mesostructure and the nature of the inorganic walls, to make a better evaluation of the uptake behavior.

Figure 5 shows the time dependence of TIRON incorporation into MP TiO_2 cubic films for two different TIRON concentrations. The uptake is slower than DHDP uptake ($\tau_{1/2} \approx 70$ and 300 min for 10^{-2} and 10^{-3} mol dm^{-3} solutions, respectively). An additional feature observed is the development of a yellow color in the solution, indicative of partial film dissolution. In dense films, no significant incorporation of the molecule or film dissolution is observed. The optimal conditions requiring incorporation without dissolution are in the range of [TIRON] $< 10^{-3}$ mol dm^{-3}. The continuously increasing aspect of the uptake vs time curves may be due to the high solubility of TIRON in water, which leads to slower incorporation. This experiment demonstrates that care should be taken when mesoporous films are exposed to ligands of potential interest that could damage the mesostructure; however, in the proper concentration conditions, functionalization is possible with low damage to the mesostructure.

Leaching Experiments. Leaching experiments are essential to assess the anchoring of the molecules incorporated into the film when exposed to different media, under simulated operation conditions (as exchangers, separators, catalyzers, ...). Unlike Si−C bonds, which are resistant toward hydrolysis or thermal treatment, the complexing groups used for grafting in this work are sensitive to nucleophilic attack by solvent. Leaching experiments were performed with titania and zirconia films functionalized by immersion in molecule solutions for varying t_{uptake} (Table 3). In the case of DHDP/TiO_2 films in THF (t_{uptake} = 4 h), ca. 20% of the incorporated DHDP is eliminated within 100 min (Figure 6); this value is unchanged after several days of exposing the functionalized film to the solvent, suggesting that the remaining DHDP is firmly attached to the pore surface. Leaching experiments in water, where DHDP is scarcely soluble, show no DHDP leaching in the explored time scale, as assessed by FTIR (Supporting Information).

The observed behavior can be explained on the basis of two different DHDP incorporation modes: strongly bound to the walls, or loosely incorporated within the pore space. It would be tempting to state that, during uptake, fast initial phosphate adsorption leads to a "strongly" bound phosphate (80% of the total DHDP); the subsequently incorporated 20% is loosely bound in the pore interior. Leaching experiments were performed with DHDP−titania films with varying t_{uptake}. Analysis of the leaching curves shows that, for low t_{uptake}

(46) (a) Hansen, E. W.; Corivaud, F.; Karlsson, A.; Kolboe, S.; Staecker, M. *Microporous Mesoporous Mater*. **1998**, *22*, 309. (b) Okazaki, M.; Toriyama, K. *J. Phys. Chem. B* **2003**, *107*, 7654.

(47) Stallmach, F.; Gräser, A.; Kärger, J.; Krause, C.; Jeschke, M.; Oberhagermann, U.; Spange, S. *Microporous Mesoporous Mater*. **2001**, *44*−*45*, 745.

Scheme 2

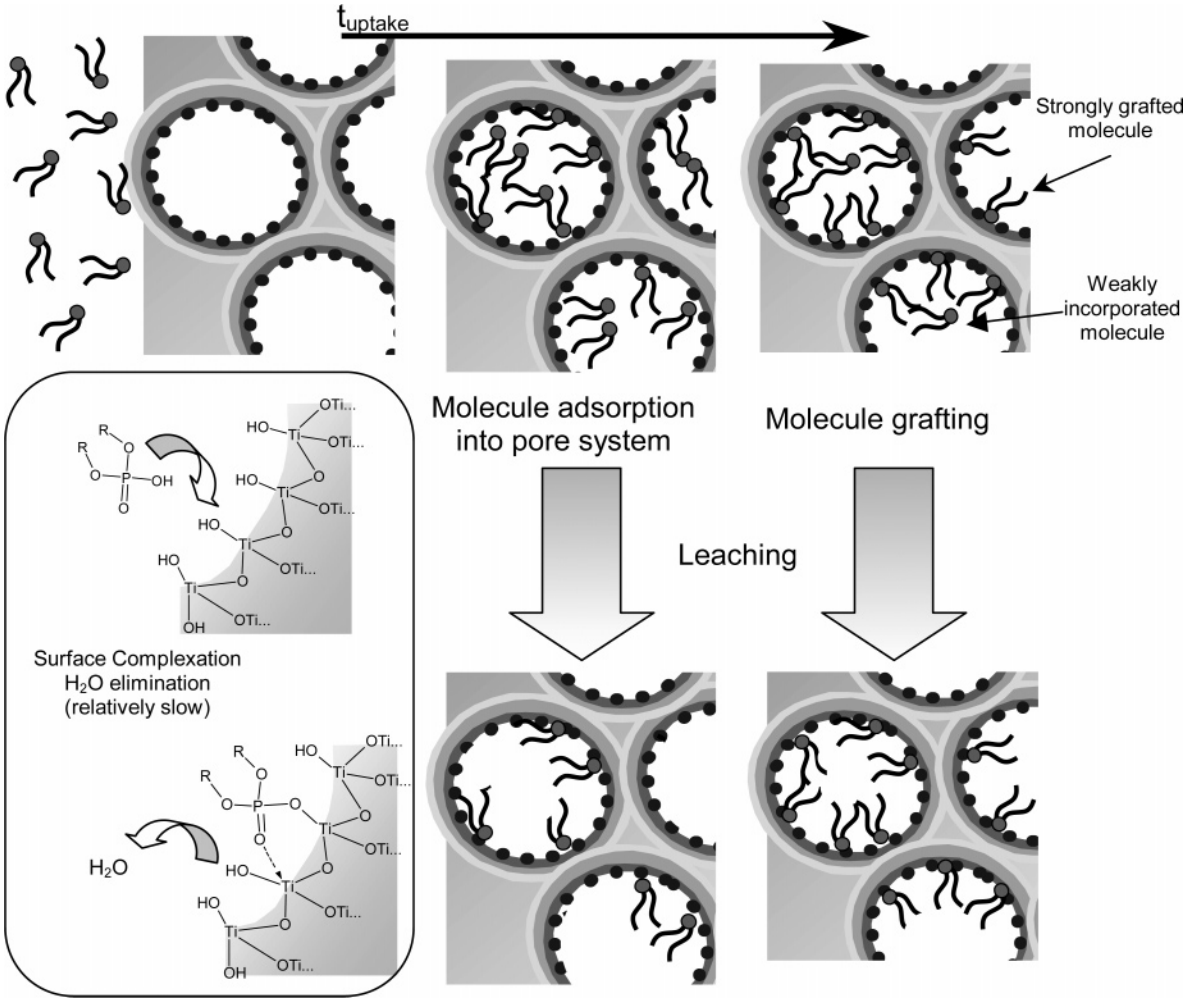

(i.e., 5−15 min, where most of the uptake is reached, Figure 4a), leaching reaches 60%. Samples submitted to leaching after higher t_{uptake} show consistently less leaching (the amount of functional molecules incorporated is not significantly higher than in the first minutes). This information suggests that the incorporation of DHDP takes place in two steps (Scheme 2): in the first one, the diffusion rate of DHDP molecules inside the pores is higher than the grafting rate; molecules quickly incorporate into the pore system, but grafting is poor. DHDP molecules inside the pores link to the oxide walls in a second step, by a surface complexation reaction. The addition of phosphate to the Ti coordination sphere implies elimination of water derived from surface hydroxyl groups; in this step, water transfer from the inorganic wall to the solvent should also play an important role in the anchoring kinetics. The surface complexation reaction generates a hybrid material with modified pore surface and firmly anchored functions (Scheme 2). In the case of other phosphate-bearing molecules such as MDP, only 10% of MDP is lost in THF within several days under agitation, for $t_{uptake} = 4$ h (Supporting Information).

TIRON leaching from titania films ($t_{uptake} = 3$ h) was followed by UV/vis spectroscopy. A 30% loss of the original content was observed at pH 5.5 (Figure 7); at lower pH values, leaching is higher (65%), and the leaching rate faster. All these observations indicate that the polyphenol anchoring

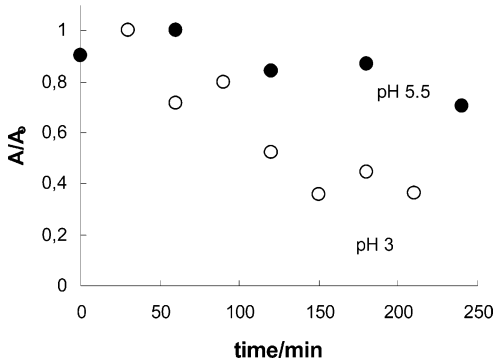

Figure 7. Time dependence of TIRON leaching from MP titania films as assessed by the decrease of the TIRON−Ti LMCT band, A_{440}. Leaching experiments were performed at pH 5.5 (●) and 3.0 (○).

groups become more labile at lower pH, most probably due to protonation of the diolate. This feature can be used in controlled delivery devices, where the release of an anchored drug can be triggered by the external pH. Dicarboxylate-grafted molecules such as 3NPA present slightly higher leaching at equivalent pH values (45% leaching in water, pH 5.5, $t = 4$ h; see the Supporting Information).

An analysis of leaching shows that there are several key factors controlling anchoring of functional groups: molecule−Ti interaction, molecule solubility in the solvent, and solvolytic capability toward the molecule−Ti complex, which includes pH. A complete set of varied behaviors (from strong

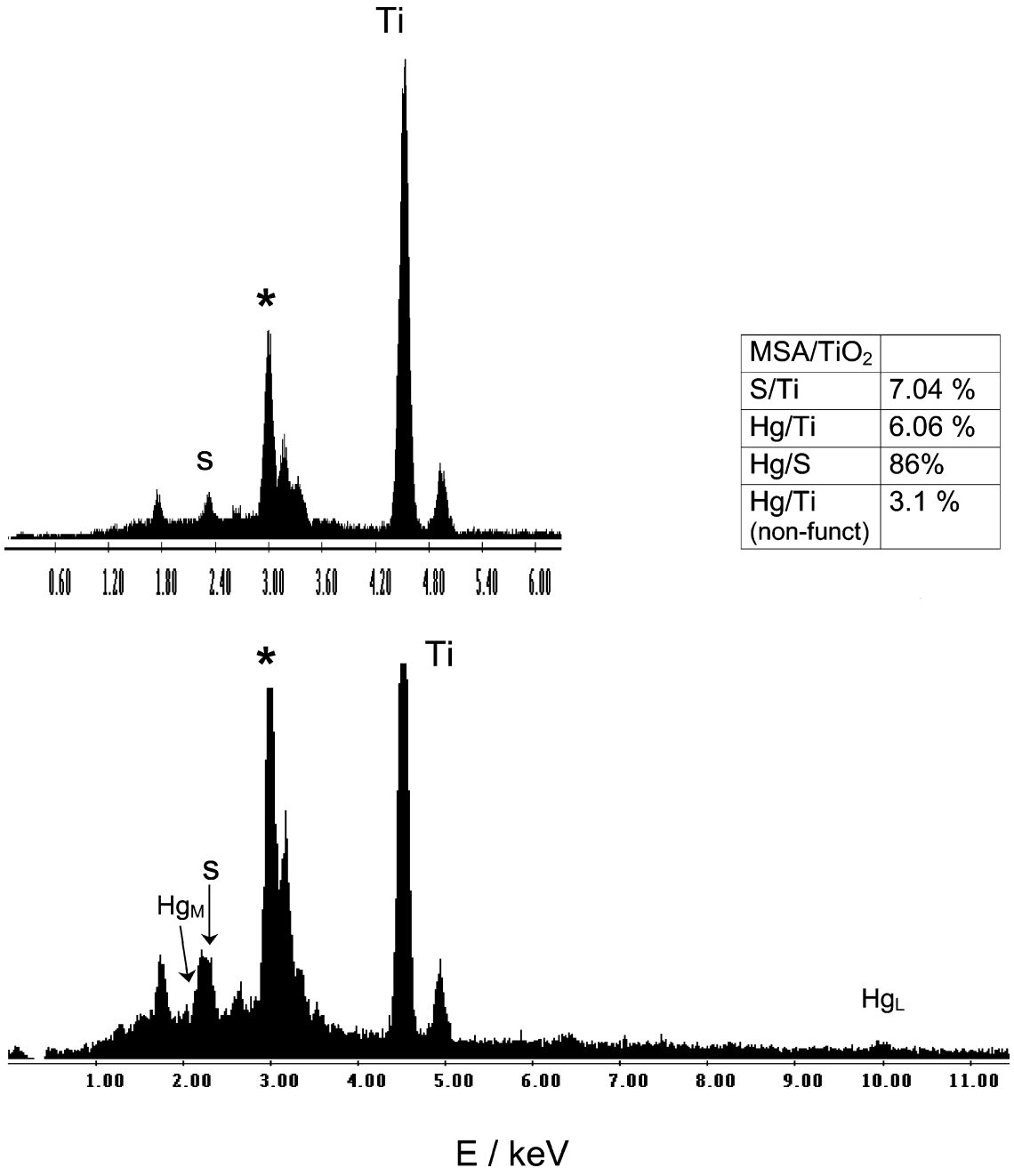

MSA/TiO_2	
S/Ti	7.04 %
Hg/Ti	6.06 %
Hg/S	86%
Hg/Ti (non-funct)	3.1 %

Figure 8. EDS spectra of MSA-functionalized MP titania films before (a, top) and after (b, bottom) exposure to 10 mM $Hg(NO_3)_2$ solutions (pH 2). Hg(II) contents have been deduced from the L and M lines; peaks marked with an asterisk are inherent to sample preparation (Au and Si from the substrate).

grafting to partial leaching to controlled leaching) can be obtained by varying the grafting strength of the group (phosphate > polyphenol > carboxylate) and the leaching solvent.

An important feature is that the pore system containing functional groups remains accessible to a second species. Figure 8 shows the EDS spectra of mercaptosuccinic acid (MSA)-functionalized TiO_2 films ($t_{uptake} = 2$ h) before and after being exposed to 10 mM $Hg(NO_3)_2$ solutions (pH 2) for 2 h. Mercury uptake is on the order of 3−9% Hg/Ti depending on the functionalizer used (cysteine, MSA, and thioglycolic acid yield 3%, 6%, and 9% Hg/Ti, respectively). The Hg/S ratio is on the order of 0.8−1, which is in good agreement with previous work done on thiol-functionalized silica powders for environmental applications.[48] Hg(II) ions tend to adsorb onto the TiO_2 surface, as well as other cations such as Cu(II) and Cd(II); an uptake of 3% Hg/Ti is observed in nonfunctionalized titania films. These cations do not adsorb on silica at these acid pH values.[49] It is interesting to remark that no significant MSA leaching occurs while the Hg(II) acid solution is in contact with the functionalized film. Analogous results (i.e., Hg-enhanced sorption and no function leaching) have been obtained using cysteine or thioglycolic acid as thiol carriers, suggesting that the anchoring of these carboxylic acids is relatively strong in these conditions.

Conclusions

In summary, we demonstrate the possibility to obtain functional MTMOs (TiO_2 and ZrO_2, but this method could

(48) Mercier, L.; Pinnavaia, T. J. *Adv. Mater.* **1997**, *9*, 500.

(49) Liu, A. M.; Hidajat, K.; Kawi, S.; Zhao, D. Y. *Chem. Commun.* **2000**, 1145.

be more generally extended to other M(IV) pure or mixed oxides), by anchoring organic groups to the pore walls of mesoporous films and xerogels. This postfunctionalization route is suitable to add organic functions to non-silica oxides. Indeed, this seems to be the most simple route to hybrid non-silica mesoporous frameworks, unless a Si−O−M network is targeted.[50] In practice, it is difficult to add organic groups by cocondensation in non-silica frameworks. This is due to the instability of most G−Ti bonding (G = grafting group) toward hydrolysis in the very acidic synthesis conditions of the films. Moreover, postfunctionalization ensures that molecules are added on the pore surface, rather than in the surface + framework.

Dramatic differences are observed for the incorporation of functions in mesoporous versus nonmesoporous solids, demonstrating that the organic functions are incorporated inside the pore system. Differences in the function incorporation are also observed depending on the mesostructure; cubic 3D mesostructures are more accessible than their 2D hexagonal counterparts. Xerogel-derived particles (particularly those with size $>2\ \mu$m) show accessibility problems, due to slow migration of molecules; strong grafting groups seem to lead to slow transport within the pore system, and could lead to pore blocking.[8] On the other hand, thin films are ideal substrates for functionalization. Grafting groups (dicarboxylate, phosphonate, phosphate, polyphenol) present a variety of behaviors toward leaching, a fact that can be further exploited for a great variety of applications (from robust selective sensors to controlled release smart materials). Indeed, MTMO surfaces can be flexibly modified with various functional groups which can be retained or liberated depending on the external conditions (pH, solvent, ...). This is a substantial difference when compared to the strong silane bonding to silica, which leads to an almost "irreversible" functionalization. Functionalized pores are further accessible to other molecules (solvent, fluorescent probes)[51] or ions (i.e., Hg(II)), opening the way for sensor or sorption applications.

Acknowledgment. We are indebted to Profs. Clément Sanchez and Sara Aldabe-Bilmes for encouraging insight and discussions. L. Pietrasanta and S. Ludueña (CMA-UBA) are thanked for the AFM and TEM images, and M. Rosenbusch is acknowledged for the SEM/EDS analysis. We thank E. Otal and M. E. Calvo for their assistance in XRD and ellipsometry; P. Morando is kindly acknowledged for his help in FTIR sample conditioning. This work was financed by CONICET/CNEA (Ph.D. grant for P.C.A.), ANPCyT (Grants PICT 06-06631, PICT 06-12057, and PICT 06-12345), Fundación Antorchas (Grant No. 14056-18), and Gabbos (Reentry Grant No. 17-P&G). 2D SAXS measurements were possible thanks to funding from LNLS, Campinas, Brazil (D11A-SAS Grant No. 2269/03). G.J.d.A.A.S.-I. is a CONICET member.

Supporting Information Available: Table and figure describing DHDP uptake as a function of the TiO_2 content in the film and figures showing the leaching of DHDP in water, MDP in THF, and 3NPA in water (PDF). This material is available free of charge via the Internet at http://pubs.acs.org.

CM048559B

(50) Soler-Illia, G. J. d. A. A.; Angelomé, P. C.; Bozzano, P. *Chem. Commun*. **2004**, 2854.

(51) Angelomé, P. C.; Marchi, M. C.; Aldabe-Bilmes, S.; Grosso, D.; Crepaldi, E. L.; Sanchez, C.; Soler-Illia, G. J. d. A. A. Work in progress.